

# Stator Flux Linkage Estimation of Synchronous Machines Based on Integration Error Estimation for Improved Transient Performance

Seunghoon Jang and Kyunghwan Choi

**Abstract**—The stator flux linkages of synchronous machines (SMs) are generally estimated by integrating their differential equations in the stationary frame. The technical challenge is removing the integration error arising from inaccurate integrator inputs and initial values. The conventional method uses a frequency domain approach to remove the integration error as a DC component by designing a high-pass filter. However, the frequency domain approach also affects irrelevant frequency components other than the DC component; thus, the magnitude or phase of the estimates could be distorted. Therefore, this study presents a novel stator flux linkage estimator for SMs, where the integration error is estimated in the time domain and subtracted from the integration result. This time domain approach does not affect other components than the integration error, guaranteeing accurate estimation. The key idea to estimating the integration error is using a linear state observer based on a circular motion of the stator flux linkages in the stationary frame. Simulation results obtained using a 35-kW SM drive demonstrate that the proposed estimator has significantly improved transient performance compared to existing methods.

**Index Terms**—Integration error, state estimation, stator flux linkage, synchronous machines (SMs), transient performance.

## I. INTRODUCTION

The electrical dynamics of synchronous machines (SMs) are described by first-order ordinary differential equations for the stator flux linkages [1]. Thus, accurate knowledge of the stator flux linkages is crucial in understanding the electrical behavior of the SM and designing a controller for the SM. For instance, model predictive control (MPC), one of the advanced control techniques based on optimization, utilizes information on the current values of the stator flux linkages or the inductances derived from them to predict the future behavior of the SM and select the optimal control action [2]. Accordingly, the accuracy of used information highly affects the performance of MPC.

Measuring the stator flux linkages inside the SM is challenging. Instead, the values of the stator flux linkages can be estimated at each steady-state operating point from the equations obtained by equating the differential equations to zero. The stator flux linkage maps can be obtained offline by an identification experiment over the entire operating range [3]. However, the map accuracy depends on the sophistication of the identification experiment at the expense of the

This work was supported by Electronics and Telecommunications Research Institute (ETRI) grant funded by the Korean government. [23ZD1160, Regional Industry ICT Convergence Technology Advancement and Support Project in Daegu-GyeongBuk (Mobility)]

S. Jang and K. Choi are with the School of Mechanical Engineering, Gwangju Institute of Science and Technology, Gwangju 61005, South Korea shjang7071@gm.gist.ac.kr; khchoi@gist.ac.kr

cost and effort. Although the stator flux linkage maps are obtained accurately for the operating range over which the experiment is performed, they cannot deal with the parameter changes resulting from aging or abnormal operations, such as temperature increase or demagnetization.

Online estimation methods have been proposed to overcome the disadvantages of offline identification. The most straightforward way was to integrate the differential equations for the stator flux linkages in the stationary  $\alpha$ - $\beta$  frame to obtain their values [4]–[6]. However, the integration suffered errors due to inaccurate initial or input values. A high-pass filter was generally applied after the integration to remove the integration errors acting as DC offsets [7], but it also distorted the frequency response around and below the cutoff frequency. A method was proposed in [8] to recover the frequency response distortion by compensating for the difference between the frequency response of the pure integrator and the filter at the frequency of the SM rotation. However, this compensation only works well under steady-state conditions that the frequency-domain approach assumes, and it would degrade transient performance.

The stator flux linkages can also be estimated in the rotating  $d$ - $q$  frame. Many studies used the steady-state assumption, by which the  $d$ - and  $q$ -axis stator flux linkages were expressed as explicit functions of the stator voltages and currents [13]–[15]. This approach is simple and easy to implement, but the transient behavior of the SM was not considered at all. The high-frequency current injection has recently been adopted for the stator flux linkage estimation [16], [17] and has shown satisfactory steady-state performance. However, their transient performance was not sufficiently investigated.

The literature shows that the existing estimation methods had poor transient performance due to the steady-state assumption, or their transient performance was not thoroughly considered in the analysis. In addition, most of them were based on conventional control methods, such as proportional-integral (PI) current control, that produced smooth control action. Their transient performance could deteriorate further if another control method that contains persistently transient components, such as finite control set MPC (FCS-MPC) [9], was adopted. Meanwhile, state observers, such as the Luenberger observer and Kalman Filter, have also been widely investigated as stator flux linkage estimators with satisfactory transient performance [10]–[12]. However, most state observer-based estimators require prior knowledge of SM electrical parameters, such as the inductances. Their steady-state or transient performance would deteriorate when

the parameter information is inaccurate.

With this background, this study presents a novel stator flux linkage estimator that does not rely on conventional estimation methods to improve transient performance. The proposed estimator is based on the conventional method: integrating the differential equations for the stator flux linkages in the  $\alpha\beta$  frame. However, the difference is in how to remove the integration error. The key idea of the proposed method is to estimate the integration error using a state observer in the time domain and subtract this error from the integration result. This time domain approach can remove the integration error faster than the conventional frequency domain approach [7], [8], which uses a high-pass filter to remove them. Note that the state observer used in the proposed method does not rely on accurate parameter information, unlike other state observer-based methods presented in [10]–[12]. Simulation results obtained using a 35-kW SM drive validate the proposed estimator's effectiveness compared to the conventional methods. FCS-MPC is selected for the current control of the SM drive to demonstrate that the proposed estimator works well even in unfavorable conditions when the stator voltages contain a wide range of frequency components.

## II. PRELIMINARIES

### A. SM Model

The SM is modeled in the stationary  $\alpha\beta$  frame as follows:

$$\dot{\lambda}_{\alpha\beta}(t) = \mathbf{v}_{\alpha\beta}(t) - R_s \mathbf{i}_{\alpha\beta}(t) \quad (1a)$$

$$T_e(t) = 1.5P (\lambda_\alpha(t)i_\beta(t) - \lambda_\beta(t)i_\alpha(t)) \quad (1b)$$

with  $\mathbf{z}_{\alpha\beta} := [z_\alpha \ z_\beta]^T$ ,  $z = \lambda, v, i$ , where  $\boldsymbol{\lambda}_{\alpha\beta}$  represents the stator flux linkage vector;  $\lambda_\alpha$  and  $\lambda_\beta$  represent the  $\alpha$ - and  $\beta$ -axis stator linkages, respectively;  $\mathbf{v}_{\alpha\beta}$  and  $\mathbf{i}_{\alpha\beta}$  represent the stator voltage and currents vectors;  $v_\alpha$  and  $v_\beta$ , and,  $i_\alpha$  and  $i_\beta$  represent the  $\alpha$ - and  $\beta$ -axis stator voltages and currents, respectively;  $R_s$  denotes the stator resistance;  $T_e$  is the output torque; and  $P$  is the number of pole pairs.

The above model is expressed differently in the rotating  $dq$  frame as follows:

$$\dot{\lambda}_{dq}(t) = \mathbf{v}_{dq}(t) - R_s \mathbf{i}_{dq}(t) - \omega_r \mathbf{J} \boldsymbol{\lambda}_{dq}(t) \quad (2a)$$

$$T_e(t) = 1.5P (\lambda_d(t)i_q(t) - \lambda_q(t)i_d(t)) \quad (2b)$$

with  $\mathbf{z}_{dq} := [z_d \ z_q]^T$ ,  $z = \lambda, v, i$ , where  $\boldsymbol{\lambda}_{dq}$ ,  $\mathbf{v}_{dq}$  and  $\mathbf{i}_{dq}$  are the physical quantities defined in the  $dq$  frame;  $\mathbf{J} := \begin{bmatrix} 0 & -1 \\ 1 & 0 \end{bmatrix}$  is the rotation matrix; and  $w_r$  is the electrical rotor speed.

The following assumptions are made in this study:

- The stator resistance  $R_s$  is known.
- The inverter nonlinearity and iron loss in the electrical dynamics are not considered.

Note that this study does not require this difficult assumption: the inductance information is accurate. Thus, the proposed stator flux linkage estimator, which will be presented in Section III, works well without accurately knowing the inductance values.

### B. Stator Flux Linkage Estimation

The stator flux linkage vector can be calculated by integrating the differential equations for them (i.e., (1a)) as follows:

$$\boldsymbol{\lambda}_{\alpha\beta}(t) = \int_0^t (\mathbf{v}_{\alpha\beta}(\tau) - R_s \mathbf{i}_{\alpha\beta}(\tau)) d\tau + \boldsymbol{\lambda}_{\alpha\beta}(0). \quad (3)$$

Because the physical quantities  $\mathbf{v}_{\alpha\beta}(t)$  and  $\boldsymbol{\lambda}_{\alpha\beta}(0)$  are not measured online in the SM drive, estimated values (denoted by hat) of them are used to estimate the stator flux linkage vector as follows:

$$\hat{\boldsymbol{\lambda}}_{\alpha\beta,int}(t) = \int_0^t (\hat{\mathbf{v}}_{\alpha\beta}(\tau) - \mathbf{R}_s \hat{\mathbf{i}}_{\alpha\beta}(\tau)) d\tau + \hat{\boldsymbol{\lambda}}_{\alpha\beta}(0). \quad (4)$$

The value of  $\hat{\mathbf{v}}_{\alpha\beta}(t)$  is determined by the stator voltage reference vector that is determined by the control logic of the SM. The initial value  $\hat{\boldsymbol{\lambda}}_{\alpha\beta}(0)$  is set to its estimated value if any, or zero. The estimated value  $\hat{\boldsymbol{\lambda}}_{\alpha\beta,int}(t)$  may contain an error due to inaccurate values of  $\hat{\mathbf{v}}_{\alpha\beta}(t)$  or  $\hat{\boldsymbol{\lambda}}_{\alpha\beta}(0)$ . Such error is defined as the integration error:

$$\boldsymbol{\Omega}_{\alpha\beta}(t) = \hat{\boldsymbol{\lambda}}_{\alpha\beta,int}(t) - \boldsymbol{\lambda}_{\alpha\beta}(t), \quad (5)$$

which acts as an offset in the estimated value. The integration error caused by an inaccurate initial value occurs at the start of the integration and remains constant. By contrast, the integration error caused by inaccurate stator voltage vector can occur continuously and change rapidly under dynamic operations of the SM. The integration error, offset in the  $\alpha\beta$  frame, is transformed into an oscillating component in the rotating  $dq$  frame, which deteriorates the stator flux linkage estimation performance both in transient and steady states.

1) *Conventional Method 1 (CM1)*: The most widely used method to remove the integration error is to apply a high-pass filter after the integration [7]. A high-pass filter, together with the integration, becomes a low-pass filter in the Laplace domain as follows:

$$\hat{\boldsymbol{\lambda}}_{\alpha\beta}(s) = \frac{1}{s + w_{c,HPF}} (\hat{\mathbf{v}}_{\alpha\beta}(s) - R_s \hat{\mathbf{i}}_{\alpha\beta}(s)), \quad (6)$$

where  $s$  is the Laplace variable and  $w_{c,HPF}$  is the cutoff frequency of the high-pass filter. The high-pass filter removes a DC offset in the integration. However, it also distorts the frequency response around and below the cutoff frequency; thus, the estimated value is distorted in its magnitude or phase, which worsens when the SM is rotating with a frequency within the distorted frequency range. The frequency response distortion can be recovered by the method presented in [8], which compensates for the difference between the frequency response of the pure integrator (i.e., (3)) and the low-pass filter (i.e., (6)) at the frequency of the SM rotation (i.e.,  $s = jw_r$ ). This compensation works well under the assumption that the low-pass filter input (i.e.,  $\hat{\mathbf{v}}_{\alpha\beta}(s) - R_s \hat{\mathbf{i}}_{\alpha\beta}(s)$ ) contain the frequency components only near  $s = jw_r$ . This assumption may not be valid when the SM is in transient conditions, or the stator voltage  $\hat{\mathbf{v}}_{\alpha\beta}(t)$  contains various frequency components due to using particular control methods such as FCS-MPC.

2) *Conventional Method 2 (CM2)*: The stator flux linkage vector can be directly estimated in the rotating  $d$ - $q$  frame under the steady-state assumption by which the derivative term in (2a) is equal to zero. Then, the estimate of the stator flux linkage vector is obtained as follows:

$$\hat{\lambda}_{dq}(t) = \frac{1}{w_r} \mathbf{J}^{-1}(\hat{v}_{dq}(t) - R_s i_{dq}(t)), \quad (7)$$

where  $\hat{v}_{dq}$  is the estimate of  $v_{dq}$ , which is determined by the stator voltage reference vector in the  $d$ - $q$  frame. This estimation works well only in steady states; thus, its performance deteriorates when the SM is in transient conditions or the stator voltage vector  $v_{dq}(t)$  keeps varying due to using particular control methods such as FCS-MPC.

### III. PROPOSED STATOR FLUX LINKAGE ESTIMATOR

This section presents a novel stator flux linkage estimator that overcomes the limitations of the abovementioned conventional methods. Instead of removing the integration error by the high-pass filter, which also affects irrelevant frequency components, the proposed estimator is based on a state observer to estimate the integration error  $O_{\alpha\beta}(t)$  in the time domain. The estimated integration error is directly compensated from the integration result  $\hat{\lambda}_{\alpha\beta,int}(t)$  so that irrelevant frequency components remain intact. Section III-A introduces a reformulation of the integration result so that the reformulated equation can be used in a state observer. Then, in Section III-B, a state observer is designed to estimate the integration error, and the overall estimation process is described.

#### A. Reformulation of Integration Result

The stator flux linkage vector can be expressed by a function of the stator current vector as follows:

$$\lambda_{\alpha\beta}(t) = \mathbf{L}_s i_{\alpha\beta}(t), \quad (8)$$

where  $\mathbf{L}_s$  denotes the inductance matrix describing a geometric relationship between  $\lambda_{\alpha\beta}$  and  $i_{\alpha\beta}$ . Note that  $\mathbf{L}_s$  is a function of  $i_{dq}$ , not of  $i_{\alpha\beta}$ . Using a nominal value for  $\mathbf{L}_s$  yields an additional term to (8) as follows:

$$\lambda_{\alpha\beta}(t) = \hat{\mathbf{L}}_s i_{\alpha\beta}(t) + \Delta\lambda_{\alpha\beta}(t), \quad (9)$$

where  $\hat{\mathbf{L}}_s$  is the nominal inductance matrix and  $\Delta\lambda_{\alpha\beta}(t) = (\mathbf{L}_s - \hat{\mathbf{L}}_s) i_{\alpha\beta}(t)$ .

The integration result  $\hat{\lambda}_{\alpha\beta,int}(t)$  is rewritten by substituting (9) into (5) as follows:

$$\hat{\lambda}_{\alpha\beta,int}(t) = \hat{\mathbf{L}}_s i_{\alpha\beta}(t) + \Delta\lambda_{\alpha\beta}(t) + O_{\alpha\beta}(t). \quad (10)$$

At steady states (i.e.,  $\mathbf{L}_s$  is constant), the terms  $\hat{\mathbf{L}}_s i_{\alpha\beta}(t)$  and  $\Delta\lambda_{\alpha\beta}(t)$  are rotating in the  $\alpha$ - $\beta$  frame with the angular velocity of  $w_r$  about different centers,  $O_{\alpha\beta}(t)$  and  $O_{\alpha\beta}(t) + \hat{\mathbf{L}}_s i_{\alpha\beta}(t)$ , respectively, as depicted in Fig. 1. On the other hand, the term  $O_{\alpha\beta}(t)$  is quasi-constant at steady states.

#### B. State Observer Design

Identification of  $\Delta\lambda_{\alpha\beta}(t)$  or  $O_{\alpha\beta}(t)$  makes it possible to identify the stator flux linkage vector  $\lambda_{\alpha\beta}(t)$  from (9)

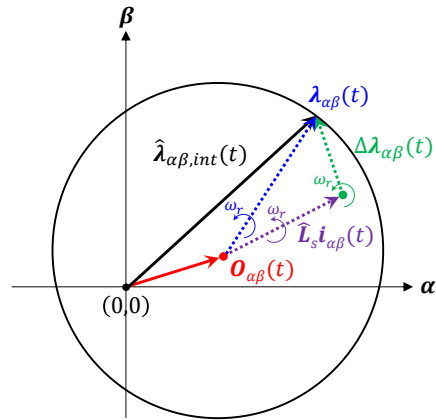


Fig. 1. Components of the integration result  $\hat{\lambda}_{\alpha\beta,int}(t)$ .

or (5), respectively. Thus, to estimate these two components  $\Delta\lambda_{\alpha\beta}(t)$  and  $O_{\alpha\beta}(t)$ , the steady-state behavior of them is modeled as follows:

$$\begin{cases} \Delta\dot{\lambda}_{\alpha\beta}(t) = w_r \mathbf{J} \Delta\lambda_{\alpha\beta}(t) \\ \dot{O}_{\alpha\beta}(t) = 0 \end{cases}. \quad (11)$$

The summation of the two components is known from (10) as

$$\hat{\lambda}_{\alpha\beta,int}(t) - \hat{\mathbf{L}}_s i_{\alpha\beta}(t) = \Delta\lambda_{\alpha\beta}(t) + O_{\alpha\beta}(t). \quad (12)$$

The state-space model is defined based on (11) and (12) as follows:

$$\begin{cases} \dot{\mathbf{x}}(t) = \mathbf{A}(\omega_r) \mathbf{x}(t) \\ \mathbf{y}(t) = \mathbf{C} \mathbf{x}(t) \end{cases} \quad (13)$$

with  $\mathbf{x} := [\Delta\lambda_{\alpha\beta} \ O_{\alpha\beta}]^T$ ,  $\mathbf{y} := \hat{\lambda}_{\alpha\beta,int} - \hat{\mathbf{L}}_s i_{\alpha\beta}$ ,  $\mathbf{A}(\omega_r) := \begin{bmatrix} w_r \mathbf{J} & \mathbf{O}_2 \\ \mathbf{O}_2 & \mathbf{O}_2 \end{bmatrix}$ ,  $\mathbf{C} := [\mathbf{I}_2 \ \mathbf{I}_2]$ , where  $\mathbf{x}$  and  $\mathbf{y}$  denote the state and output vectors, and,  $\mathbf{A}(\omega_r)$  and  $\mathbf{C}$  represent the system and output matrices, respectively.

The observability matrix of the state-space model (13) is given by

$$\mathcal{O}(\omega_r) = \begin{bmatrix} \mathbf{C} \\ \mathbf{C}\mathbf{A}(\omega_r) \\ \mathbf{C}\mathbf{A}(\omega_r)^2 \\ \mathbf{C}\mathbf{A}(\omega_r)^3 \end{bmatrix} = \begin{bmatrix} \mathbf{I}_2 & \mathbf{I}_2 \\ \omega_r \mathbf{J} & \mathbf{O}_2 \\ (\omega_r \mathbf{J})^2 & \mathbf{O}_2 \\ (\omega_r \mathbf{J})^3 & \mathbf{O}_2 \end{bmatrix}, \quad (14)$$

which has full rank (i.e.,  $\mathcal{O}(\omega_r) = 4$ ) if  $\omega_r \neq 0$ . Consequently, the state  $\mathbf{x}$  is fully observable at nonzero speeds. A linear state observer for the state-space model is designed as follows:

$$\begin{cases} \dot{\hat{\mathbf{x}}}(t) = \mathbf{A}(\omega_r) \hat{\mathbf{x}}(t) + \mathbf{F}(\mathbf{y}(t) - \hat{\mathbf{y}}(t)) \\ \hat{\mathbf{y}}(t) = \mathbf{C} \hat{\mathbf{x}}(t), \end{cases} \quad (15)$$

where  $\hat{\mathbf{x}}$  and  $\hat{\mathbf{y}}$  are the estimates of  $\mathbf{x}$  and  $\mathbf{y}$ , respectively, and

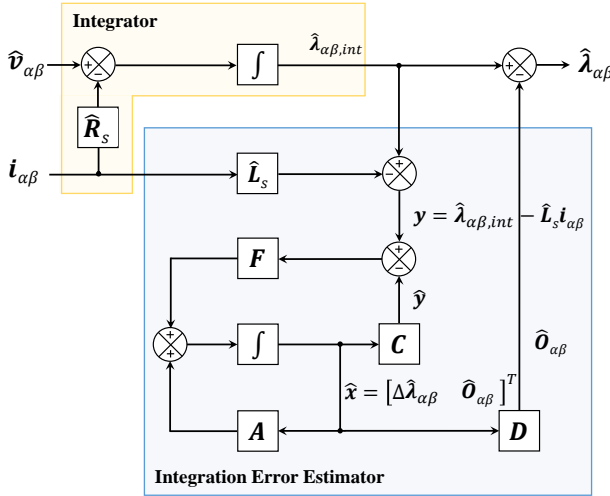


Fig. 2. Proposed stator flux linkage estimator.

TABLE I  
SPECIFICATIONS OF THE PMSM DRIVE MODEL

Base speed	2000 RPM
Maximum torque	180 Nm
DC-link voltage	325 V
Maximum stator current	350 A
Sampling time	25 $\mu$ s
Number of pole pairs ( $P$ )	8
Stator resistance ( $R_s$ )	10.9 m $\Omega$

$F$  is the observer gain matrix. The estimation error dynamics can be obtained by subtracting (15) from (13) as follows:

$$\dot{e}(t) = [\mathbf{A}(\omega_r) - \mathbf{FC}] e(t), \quad (16)$$

where  $e = x - \hat{x}$ . The estimation error  $e(t)$  asymptotically and exponentially converges to zero if the observer gain matrix  $F$  is determined to make the matrix  $\mathbf{A}(\omega_r) - \mathbf{FC}$  Hurwitz.

Finally, the estimate of the stator flux linkage vector  $\hat{\lambda}_{\alpha\beta}(t)$  is obtained by subtracting the integration error estimator  $\hat{\mathbf{O}}_{\alpha\beta}(t)$  from the integration result  $\hat{\lambda}_{\alpha\beta,int}$ :

$$\hat{\lambda}_{\alpha\beta} = \hat{\lambda}_{\alpha\beta,int} - \hat{\mathbf{O}}_{\alpha\beta} = \hat{\lambda}_{\alpha\beta,int} - \mathbf{D}\hat{x}, \quad (17)$$

where  $\mathbf{D} := [\mathbf{O}_2 \quad \mathbf{I}_2]$ . This process is depicted in Fig. 2. The estimate in the  $\alpha\beta$  frame is transformed into that in the rotating  $d-q$  as follows:

$$\hat{\lambda}_{dq} = \mathbf{T}(\theta_r)\hat{\lambda}_{\alpha\beta}. \quad (18)$$

where  $\mathbf{T}(\theta_r)$  is the coordinate transformation matrix and  $\theta_r$  is the electrical rotor position.

#### IV. SIMULATION RESULTS

MATLAB/SIMULINK simulations were performed to verify the effectiveness of the proposed stator flux linkage estimator over a wide range of speeds. A 35-kW permanent magnet SM (PMSM) drive model was used in the simulations, whose specifications and stator flux linkage maps

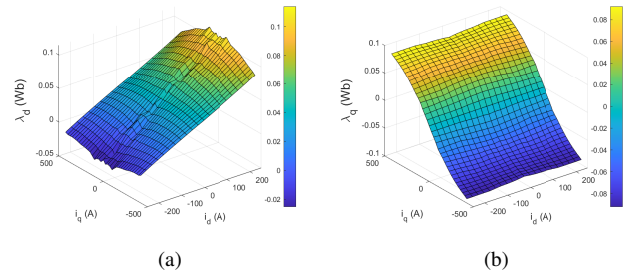


Fig. 3. Stator flux linkage maps of the PMSM. (a)  $d$ -axis and (b)  $q$ -axis.

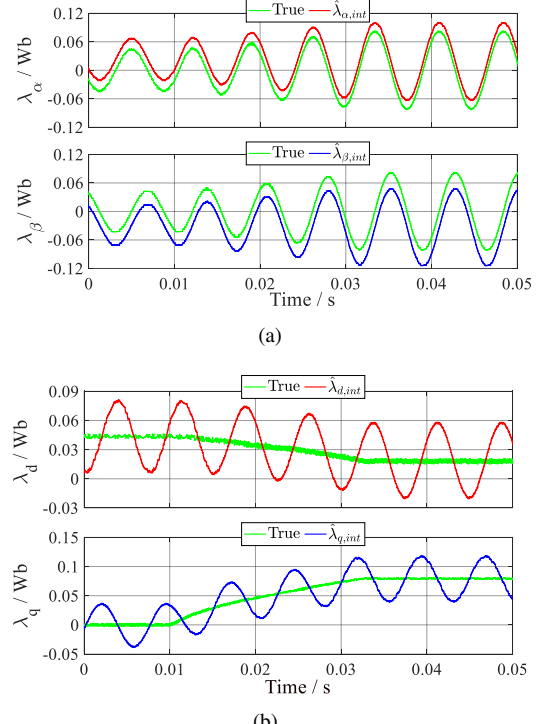


Fig. 4. Stator flux linkage estimates (a) in the  $\alpha\beta$  frame and (b) in the  $d-q$  frame without using the integration error estimator.

are given in Table I and Fig. 3, respectively. A PI speed controller was designed to determine the desired speed for the PMSM to track the speed command. The desired speed was then converted to current references based on maximum torque per ampere (MTPA) operation using the numerical method presented in [18]. Finally, FCS-MPC determined the stator voltage references for the PMSM to track the current references [9]. Note that FCS-MPC was selected for the current control to make the stator voltages contain a wide range of frequency components.

The simulations consisted of two parts. In the first part (see Section IV-A), the effectiveness of the integration error estimator was examined by comparing estimation results with and without the integration error estimator. When the integration error estimator was not used, the estimate of the stator flux linkage vector was determined as  $\hat{\lambda}_{\alpha\beta}(t) = \hat{\lambda}_{\alpha\beta,int}(t)$  in the  $\alpha\beta$  plane, unlike in (17). The PMSM was controlled to produce the maximum torque (180 Nm) at the

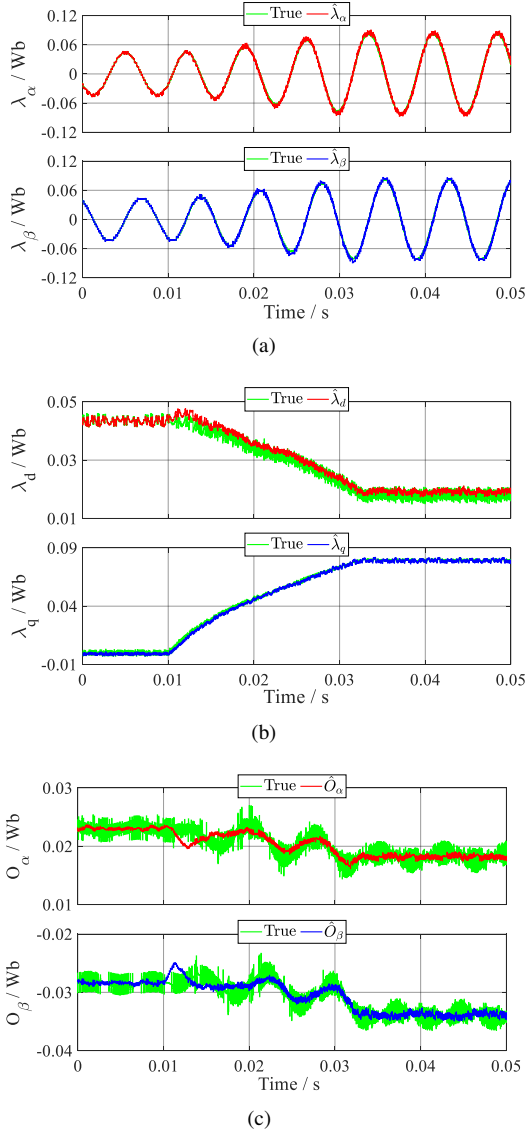


Fig. 5. Stator flux linkage estimates (a) in the  $\alpha$ - $\beta$  frame and (b) in the  $d$ - $q$  frame using the integration error estimator. (c) The corresponding integration error estimates.

mechanical speed of 1000 RPM. In the second part (see Section IV-B), the proposed estimator (with the integration error estimator), which was termed the proposed method (PM), was compared with two conventional methods: CM1 (see Section II-B.1) and CM2 (see Section II-B.2). The estimates of CM1 were transformed into the  $d$ - $q$  frame to match the coordinate to PM. The cutoff frequency of the high-pass filter of CM1 was selected as  $0.2w_r$  which did not significantly affect the operating point (i.e.,  $s = w_r$ ). The estimates of CM2 were low-pass filtered with a cutoff frequency of  $2w_r$  to filter out high-frequency components generated by FCS-MPC, considering the estimation performance. Note that the cutoff frequencies of CM1 and CM2 were optimally tuned by a prior simulation. The nominal inductance matrix of PM was defined as  $\hat{\mathbf{L}}_s = 2.8 \cdot 10^{-6} \mathbf{I}_2(\text{H})$ , where the value of the diagonal terms was selected as the average value of the  $d$ -

and  $q$ -axis nominal inductances. Additionally, the observer gain matrix  $\mathbf{F}$  of PM was selected such that the eigenvalues of the matrix  $A(\omega_r) - \mathbf{F}\mathbf{C}$  match with the bandwidth of the current reference, which was 50 Hz, at the mechanical speed of 1000 RPM. The PMSM was controlled to produce torque from -180 Nm to 180 Nm within a mechanical speed range of 200 RPM to 1800 RPM.

#### A. Validation of the Integration Error Estimator

The estimation results without and with the integration error estimator are presented in Figs. 4 and 5, respectively. Figure 4a shows that the estimates in the  $\alpha$ - $\beta$  frame tracked the trend of the true values. However, the estimates had offsets from inaccurate integration. Figure 4b shows that the offsets in the  $\alpha$ - $\beta$  frame were transformed into oscillating components in the rotation  $d$ - $q$  frame, which deteriorated the estimation performance.

By contrast, Fig. 5a shows that the estimates in the  $\alpha$ - $\beta$  frame tracked the true values accurately with the integration error estimator. Accordingly, the estimates in the  $d$ - $q$  frame also tracked the true values accurately, as shown in Fig. 5b. This accurate estimation was possible because the integration error was estimated, as shown in Fig. 5c, and compensated from the integration result in real time.

#### B. Performance Comparison with Conventional Methods

Figure 6 shows the stator flux linkage estimates of PM, CM1, and CM2 in the  $d$ - $q$  frame, as well as the integration error of PM, as the torque and mechanical speed were varying. The estimates of CM1 reached the true values without overshoots and oscillations in steady states over 1000 RPM. However, they had overshoots and oscillations at low-torque and low-speed conditions (from 0.05 s to 0.12 s) and did not converge to the true values. These overshoots and oscillations occurred because the integration error could not be removed rapidly using the frequency domain approach.

The estimates of CM2 reached the true values in steady states over 1000 RPM. However, the  $d$ -axis estimate had a large initial overshoot when the torque was varying at around 200 RPM (from 0.05 s to 0.08 s) due to not considering the transient terms in (2a). The overshoot could be attenuated by decreasing the low-pass filter's cutoff frequency, but this would increase the settling time of the  $d$ - and  $q$ -axis estimates.

By contrast, the estimates of PM tracked the true values well both in transient and steady states at all speeds, which was possible due to using the integration error estimator to remove the integration error in the time domain. Therefore, it is demonstrated that the proposed stator flux linkage estimator significantly improves the transient and steady-state performance compared to the conventional estimation methods over a wide range of speeds.

## V. CONCLUSION

This study presented a time domain approach to more accurately estimate the stator flux linkages of SMs than the conventional frequency domain approach. The main

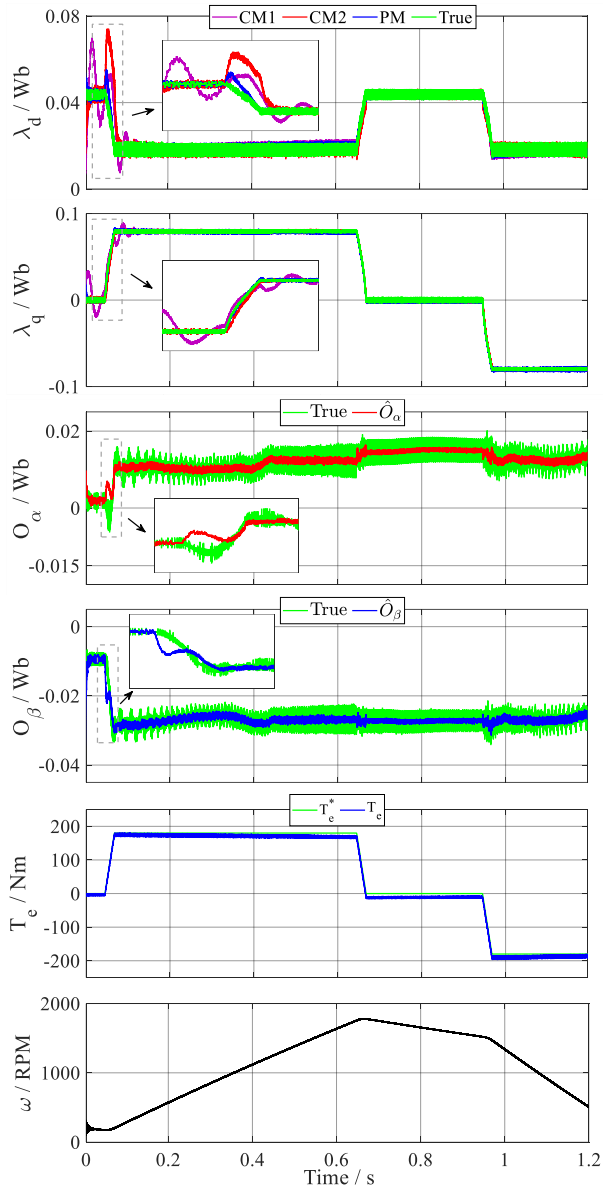


Fig. 6. Stator flux linkage estimates of the proposed method (PM) and conventional methods (CM1 and CM2) in the  $d$ - $q$  frame.

challenge was to eliminate the integration error existing in the integration result of the differential equations for the stator flux linkages. The key idea of the proposed method was to estimate the integration error in the time domain using a linear state observer and compensate for this error from the integration result. The state observer was designed by leveraging the fact that the stator flux linkage vector is in a circular motion in the  $\alpha$ - $\beta$  frame. Simulation results obtained using a 35-kW PMSM drive demonstrated that the proposed estimator closely tracked the true trajectories of the stator flux linkages under various operating conditions with better transient performance than the conventional estimators. In a future study, the proposed estimator will be validated by experimental results considering non-ideal factors, which were neglected in this study, such as inverter nonlinearities

that may significantly affect the estimation accuracy.

## REFERENCES

- [1] S.-K. Sul, *Control of electric machine drive systems*. John Wiley & Sons, 2011.
- [2] G. P. Karamanakos, E. Liegmann, T. Geyer, and R. Kennel, "Model predictive control of power electronic systems: Methods, results, and challenges," *IEEE Open Journal of Industry Applications*, vol. 1, pp. 95-114, 2020.
- [3] E. Armando, R. I. Bojoi, P. Guglielmi, G. Pellegrino, and M. Pastorelli, "Experimental identification of the magnetic model of synchronous machines," *IEEE Transactions on Industry Applications*, vol. 49, no. 5, pp. 2116-2125, 2013.
- [4] L. Tang, L. Zhong, M. F. Rahman, and Y. Hu, "A novel direct torque controlled interior permanent magnet synchronous machine drive with low ripple in flux and torque and fixed switching frequency," *IEEE Transactions on Power Electronics*, vol. 19, no. 2, pp. 346-354, 2004.
- [5] Y. Inoue, S. Morimoto, and M. Sanada, "Examination and linearization of torque control system for direct torque controlled IPMSM," *IEEE Transactions on Industry Applications*, vol. 46, no. 1, pp. 159-166, 2009.
- [6] Y. Inoue, S. Morimoto, and M. Sanada, "Comparative study of PMSM drive systems based on current control and direct torque control in flux-weakening control region," *IEEE Transactions on Industry Applications*, vol. 48, no. 6, pp. 2382-2389, 2012.
- [7] M. Hinkkanen and J. Luomi, "Modified integrator for voltage model flux estimation of induction motors," *IEEE Transactions on Power Electronics*, vol. 50, no. 4, pp. 818-820, Aug. 2003.
- [8] A. Choudhury, P. Pillay, and S. S. Williamson, "Modified stator flux estimation based direct torque controlled PMSM drive for hybrid electric vehicle," in *IECON 2012-38th Annual Conference on IEEE Industrial Electronics Society*, pp. 2965-2970, IEEE, 2012.
- [9] J. Rodriguez et al., "Predictive current control of a voltage source inverter," *IEEE Transactions on Industrial Electronics*, vol. 54, no. 1, pp. 495-503, 2007.
- [10] Y. Sun, S. Yan, B. Cai, Y. Wu, and Z. Zhang, "MPPT adaptive controller of DC-based DFIG in resistances uncertainty," *International Journal of Control, Automation and Systems*, vol. 19, no. 8, pp. 2734-2746, 2021.
- [11] E. Salman and M. Yilmaz, "A Novel Sensorless Control Approach for IPMSM Using Extended Flux Based PI Observer for Washing Machine Applications," *International Journal of Control, Automation and Systems*, vol. 21, no. 7, pp. 2313-2322, 2023.
- [12] Q.-M. Wu, Y. Zhan, M. Zhang, X.-P. Chen, and W.-P. Cao, "Efficiency optimization control of an IPMSM drive system for electric vehicles (EVs)," *International Journal of Control, Automation and Systems*, vol. 19, no. 8, pp. 2716-2733, 2021.
- [13] T. Sun, J. Wang, M. Koc, and X. Chen, "Self-learning MTPA control of interior permanent-magnet synchronous machine drives based on virtual signal injection," *IEEE Transactions on Industry Applications*, vol. 52, no. 4, pp. 3062-3070, 2016.
- [14] T. Sun, M. Koc, and J. Wang, "MTPA control of IPMSM drives based on virtual signal injection considering machine parameter variations," *IEEE Transactions on Industrial Electronics*, vol. 65, no. 8, pp. 6089-6098, 2017.
- [15] Y. Miao, H. Ge, M. Preindl, J. Ye, B. Cheng, and A. Emadi, "MTPA fitting and torque estimation technique based on a new flux-linkage model for interior-permanent-magnet synchronous machines," *IEEE Transactions on Industry Applications*, vol. 53, no. 6, pp. 5451-5460, 2017.
- [16] M. Martinez, D. Reigosa, D. Fernandez, J. M. Guerrero, and F. Briz, "Enhancement of permanent magnet synchronous machines torque estimation using pulsating high frequency current injection," *IEEE Transactions on Industry Applications*, 2019.
- [17] D. F. Laborda, D. D. Reigosa, D. Fernández, K. Sasaki, T. Kato, and F. Briz, "Enhanced torque estimation in variable leakage flux PMSM combining high and low frequency signal injection," *IEEE Transactions on Industry Applications*, vol. 59, no. 1, pp. 801-813, 2022.
- [18] K. Choi, Y. Kim, K.-S. Kim, and S.-K. Kim, "Real-time optimal torque control of interior permanent magnet synchronous motors based on a numerical optimization technique," *IEEE Transactions on Control Systems Technology*, vol. 29, no. 4, pp. 1815-1822, 2020.